Dalton Transactions

Accepted Manuscript

ROYAL SOCIETY OF CHEMISTRY

www.rsc.org/dalton

Benchmark study of Mössbauer isomer shifts of Eu and Np complexes by relativistic DFT calculation for the understanding of bonding nature of f-block compounds

Masashi Kaneko,[a] Sunao Miyashita,[a] and Satoru Nakashima*[b]

[a]Graduate School of Science, Hiroshima University

[b]Natural Science Center for basic Research and Development, Hiroshima University

E-mail: snaka@hiroshima-u.ac.jp

Abstract

We have performed the benchmark investigations about the bonding properties in lanthanide and actinide complexes to estimate quantitatively the covalency of f-block compounds. Three different density functionals including BP86 (pure-GGA), B3LYP (hybrid-GGA) and B2PLYP (double hybrid-GGA) were employed to all-electron self-consistent field calculations compensated by scalar-relativistic zero-order regular approximation (ZORA) Hamiltonian with relativistically contracted all-electron basis set. Ten Eu and ten Np complexes were employed as benchmark sets for the calculation of Mössbauer parameters for ^{151}Eu and ^{237}Np compounds. As the result of the linear fitting between calculated electron densities at nucleus (ρ_0^{calc}) and experimental isomer shifts (δ^{exp}), the calculation performed by all-electron ZORA-B2PLYP level reproduced the change of electronic density at Mössbauer nucleus for both Eu and Np complexes with high correlation coefficients ($R^2 >$ 0.90). Mulliken's population analyses indicated that BP86 and B3LYP methods overestimated the covalency of both Eu and Np complexes due to smaller amount of the exact Hartree-Fock exchange admixture included in BP86 and B3PLYP compared to that in B2PLYP functional. By comparing Mulliken's electronic structure analyses with experimental isomer shifts, we found that Mulliken's spin population values were good parameters to estimate quantitatively the bonding natures for Eu and Np complexes.

1. Introduction

Density functional theory (DFT) is one of the most useful tools for the investigations of electronic states, bonding and molecular orbitals in f-element compounds.[1-3] The f-elements computational chemistry at a molecular-level study has fascinated many chemists from the point of both fundamental and applied chemistries. The former case mainly includes the diversity of reactivities and geometries in lanthanide (Ln) / actinide (An) compounds. In the latter case the separation of minor actinide including Am^{3+} and Cm^{3+} from lanthanide in the high-level radioactive

liquid waste has been investigated for solving a challenging nuclear waste problem. In both cases, it has been pointed that how f-electrons contribute to their electronic and/or bonding states is a common key problem.

Mössbauer spectroscopy has been employed to research the hyperfine interaction between Mössbauer nucleus and its environment. The results obtained by Mössbauer experiments have revealed the electron density at the nucleus (ρ_0) relative to source and the distribution of valence electrons around its nucleus in compounds corresponding to isomer shift (δ) and quadrupole splitting (ΔE_Q) values, respectively. Since Mössbauer effects can be observed in ^{151}Eu and ^{237}Np nuclei, the detailed discussion about the bonding of f-block complexes has been developed. A couple of particular investigations about the covalency of lanthanide and actinide complexes were reported. Long and co-workers[4] suggested the evidence of the covalent interaction in a [$Eu^{III}Cp_3$(THF)] (Cp = η^5-C_5H_5; THF = tetrahydrofuran) complex and Karraker *et al.*[5] revealed the change in covalency in [$Np^{IV}Cp_3X$] (X = Cl, alkoxy, *p*-$CH_3C_6H_4CH_2$, alkyl) complexes. In both cases, it was a probable reason that the covalent contribution of f-electrons to bonding influenced the monopole interaction between its nucleus and neighbor electrons.

Mössbauer isomer shift values were formulated as the difference between electron densities at nuclear position of absorber ($\rho_0^{absorber}$) and source (ρ_0^{source}) multiplied by the constant coefficient depending on only Mössbauer nuclides (Eq. 1)

$$\delta = \{(4\pi/5)\, Ze^2R^2\, (\Delta R/R)\}\, (\rho_0^{absorber} - \rho_0^{source}) \qquad (1)$$

where e is the elementary electric charge, Z and R are the nuclear charge and its radius, respectively, and ΔR is the variation of the nuclear radius between Mössbauer transition states.[6] The connection of Mössbauer isomer shift with DFT can be achieved by the linear relationship between δ and ρ_0 values (Eq. 2)

$$\delta^{exp} = a\, (\rho_0^{calc} - b) \qquad (2)$$

where δ^{exp} and ρ_0^{calc} are the experimental δ value and the calculated ρ_0 value for the target compounds, respectively, a and b are the constants fitted by the relationship between δ^{exp} and ρ_0^{calc}. Previous benchmark studies for ^{57}Fe isomer shifts were reported successfully.[7-15] As pointed by Filatov *et al.*,[16-20] this formalism was, however, based on some assumptions that the electron inside nucleus was constant and did not depend on the variation of nuclear radius during γ–ray resonance. And the consideration of a finite nucleus model during the calculation of variational energy, such as a self-consistent field calculation, was important for relativistic quantum calculation. In order to solve these problems, Filatov *et al.* have developed more accurate treatment for the prediction of isomer shift values by employing the linear response theory.[16-20] However, such benchmark studies for ^{151}Eu and ^{237}Np systems have never reported.

Owing to the application of relativistic approximation to Kohn-Sham equation, the discussion about the reactivity and the bonding of f-block complexes has been reported by using a relativistic

DFT calculation. Applying the all-electron MO calculation with scalar relativistic treatment, Kaltsoyannis *et al.* have revealed that the covalency in $[An^{IV}Cp_4]$ (An^{IV} = Th, Pa, U, Np, Pu, Am and Cm) complexes could be correlated with the molecular orbital and the bond critical point analyses.[21] More recently, as the research for the selective separation of minor actinides, Belkhiri and co-workers published that the selectivity of minor actinide from lanthanides was attributed to the difference in bonding of f-electrons, however, the dependency of bonding energy on functionals was also observed.[22] This intrinsic character in the framework of DFT has limited us to the qualitative prediction of its covalency. Therefore, the universal method to quantitatively predict simultaneously the covalency of both lanthanide and actinide complexes has been desired intensely.

In the present study, for the purpose of the quantitative discussion about the bonding in f-block complexes, we performed the benckmark studies for Eu and Np complexes between Mössbauer isomer shifts and calculated electron densities at nucleus position. We believe that this attempt is valuable for the estimation of the validity for the relativistic calculation, although the application of conventional formalism (eq. 1) to these relativistic systems should be considered. We also carried out the Mulliken's electronic structure analysis. We expected that the present work makes substantial contributions to not only the theoretical f-block chemistry but also the selective separation problem of minor actinides.

2. Computational details

All DFT calculations were performed by using program package *ORCA 3.0*[23] developed by Neese. Scalar-relativistic correction was considered by zero-order regular approximation (ZORA) Hamiltonian including atomic model potential, which was modified by s-type Gaussian atomic density.[24] All-electron Gaussian-type orbitals were employed as basis functions in all SCF calculations. The calculation of Mössbauer parameters unconditionally requires all-electron basis set since it needs the information of the electron density at the nucleus position. Segmented all-electron relativistically contracted (SARC) basis sets were employed for Eu $(61^{17}/51^{11}/41^{8}/41^{2})$[25], Np $(61^{16}/51^{10}/61^{7}/41^{2})$[26] atoms. All-electron relativistically contracted basis sets were assigned to all other elements augmented by one set of polarization function at triple-zeta valence level for some period 3 elements and split-valence level for some period 2 elements and the hydrogen atom.[26] We used the relativistic all-electron basis set adapted to ZORA Hamiltonian, because these basis sets need to be optimized for the specific relativistic Hamiltonian employed in SCF calculation[28]. All SCF calculations were achieved with the total energy of a convergence tolerance of 10^{-8} hartree using the resolution of the identity (RI) approximation. Geometry optimizations were performed by the quasi-Newton method at ZORA-BP86 level without any structural constraints. Single point calculations were carried out by applying three functionals (BP86, B3LYP and B2PLYP). In order to increase the radial integration accuracy for Eu and Np atoms for the purpose of describing accurately

Mössbauer atom, the special grids set to the integration accuracy of 14 were constructed to the center metal ions. Mulliken's population analyses were performed to understand the electronic structures based on LCAO-MO theory for f-block compounds.[29] Three-dimensional description of optimized structures was performed by program *VESTA*.[30]

Ten Eu and ten Np complexes were employed as the benchmark sets (Table 1). Typical trivalent Eu complexes,[32,33] which were 2,2'-bipyridine (bipy), 1,10-phenanthroline (phen) and β-diketonato complexes [$Eu^{III}L_3(H_2O)_2$] (L = acetylacetonato (acac), 1,1,1,2,2,3,3-heptafluoro-7,7-dimethyl-4,6-octanedionato (pta)), and organo-europium complexes[4,31] were included in Eu benchmark complexes. Typical isomer shifts of trivalent Eu complexes are ca. 0.3 mm s^{-1}, while organo-Eu complexes have more negative shifts of 0.06 and –1.77 mm s^{-1} for [$Eu^{III}CpCl_2(THF)_3$] and [$Eu^{III}Cp_3(THF)$], respectively. Since small δ_{Eu} values are attributed to the increase of electron density at nucleus from the fact that divalent Eu complexes have –12 ~ –13 mm s^{-1} isomer shifts, it has been suggested that those organo-Eu(III) complexes have the larger electron density by the electron donation from the ligands than nitrito, acetato and β-ketonato complexes. In the Np system, only organometallic complexes were considered as benchmark complexes including $[Np^{III/IV}(COT)]^{-/0}$ (COT^{2-} = cyclooctatetraenyl) complexes[43] and several [$Np^{IV}Cp_3X$] complexes.[5,44] All calculation models were referenced to the isostructural complexes or the properly modified structures to X-ray coordinates.

3. Results and discussion

3.1. Equilibrium structures

Spin septet and octet states were obtained as the most stable electronic ground state to other spin states for trivalent and divalent Eu complexes, respectively. Obtained structures were confirmed as the local minima by the vibrational frequencies analysis. Three-dimensional descriptions of equilibrium structures of Eu complexes were shown in Figure 1. All optimized geometries for Eu complexes were obtained as similar structures to the experiments. The key bond lengths of selected complexes were compared with the X-ray structures in Table 2. When the structure of Eu complex was not reported, the structure of Sm or Gd was used. Since the differences in the ionic radii among Sm^{3+}, Eu^{3+} and Gd^{3+} for six-coordinate systems are small (ca. ±0.01 Å), these results indicated that the calculated bond lengths were slightly overestimated by ~ 0.1 Å compared with the experimental data.

In Np system, we obtained that the electronic ground states for quadrivalent and trivalent Np complexes were spin quartet and quintet states, respectively. All equilibrium geometries of Np complexes were shown in Figure 2. The key bond lengths of Np benchmark complexes were summarized in Table 3. When the structure of Np complex was not reported, the structure of Ce or U was used. As with the Eu complexes, BP86 / SARC geometrical calculation overestimated slightly

the metal-ligand distances compared with the X-ray structures, but this method could enable us to predict the valid equilibrium structures for both Eu and Np complexes.

3.2. Benchmark studies between Mössbauer isomer shifts (δ^{exp}) and calculated electron densities at nucleus (ρ_0^{calc})

Benchmark results of ^{151}Eu isomer shifts using several functionals were shown in Figure 3 and Table 4. In any methods, the slope by the linear fitting between experimental δ_{Eu} and calculated ρ_0 was a positive value. These results were consistent with the experimental fact that the (ΔR / R) value in Eq. 1 determining the sign of the correlation between δ and ρ_0 was the positive value ($+5 \times 10^{-4}$).[52] The results of the correlation coefficients and the root mean square deviations (RMSD) revealed that the reproducibility of ^{151}Eu isomer shifts increased in the order of BP86, B3LYP and B2PLYP corresponding to pure, hybrid and double hybrid functionals, respectively. In particular, B2PLYP method including the hybrid HF&DFT exchange and the hybrid MP2&DFT correlation energies gave us the excellent agreement with the experimental results with high correlation coefficient and low RMSD values compared with BP86 and B3LYP methods. The main reason for the inconsistency of BP86 and B3LYP methods was the underestimation of the electron densities at nucleus in organo-europium complexes. For example, the calculated isomer shifts of $Eu^{III}Cp_3(THF)$ complex by the fitting parameters a and b were –4.77, –4.71 and –1.36 mm s^{-1} for BP86, B3LYP and B2PLYP functional, respectively, while its experiment isomer shift was –1.77 mm s^{-1}. Since the estimation of the bonding interaction between Eu atom and ligands should mainly attribute to the exchange interaction among electrons, it might be suggested that the mixing parameter of the HF exchange energy in B2PLYP (53 %) was appropriate to calculate the accurate description of the bonding nature in Eu complexes compared with those of BP86 (0 %) and B3LYP (20 %). We also have investigated the performance of other functionals to the smaller benchmark set (Table S1-2, Figure S1). As expected, we obtained that that the hybrid functionals with HF exchange closer to 50% without MP2 correction give the almost same correlation with experiment compared to B2PLYP functional.

Calculated ρ_0 and δ_{Np} values of Np complexes were summarized in Table 5. All methods reproduced the negative ΔR / R value observed experimentally (-1.1×10^{-4}).[53] The results of correlation coefficient and RMSD values suggested that the B2PLYP / SARC method was the most suitable for the ^{237}Np isomer shift calculation as observed in ^{151}Eu system. This result revealed that the B2PLYP functional was the universal method to reproduce the bonding nature in both lanthanide and actinide complexes. Neese *et al.*[11] and Firatov *et al.*[19] also reported that B2PLYP functional was better choice for ^{57}Fe benchmark study. As mentioned above, these results imply that the Hartree-Fock exchange admixture of 53 % in B2PLYP functional was important for the quantitative description of the covalent interaction in Np complexes. However, the calculated δ_{Np} value of $NpCp_4$ (14.7 mm s^{-1}) was deviated largely from the experiment (7.2 mm s^{-1}), although its deviation was

smaller than that of BP86 or B3LYP. The plot between experimental δ_{Np} and calculated ρ_0 was shown in Figure 4. The relative ρ_0^{calc} values to the experiment isomer shifts except $NpCp_4$ hardly depended on the methods employed, while only ρ_0 value for $NpCp_4$ increased in the order of BP86, B3LYP and B2PLYP functional. This result also suggested that the inconsistency at BP86 or B3LYP originated from the overestimation of their covalent interactions because the larger were the isomer shifts, the higher was the covalency in ^{237}Np system.

3.3. Mulliken's population analyses

In the above discussion, we showed the calculation validity to the electronic state in the vicinity of Eu and Np nuclei for their complexes. Here, we focused on the Mulliken's atomic charge and spin population analyses implemented in general DFT calculation packages to estimate the atomic electronic state in Eu and Np complexes. Atomic charges and spin populations in Eu and Np atoms were shown in Figures 5 and 6, respectively. Compared among the calculated values, BP86 and B3LYP results were smaller for atomic charges and larger for spin populations than B2PLYP results. Since B2PLYP functional can reproduce the experimental isomer shifts more than BP86 and B3LYP functionals, we suggested that the electronic structure analyses by BP86 and B3LYP methods overestimated the electronic interaction between metal atom and ligands. When focusing on the correlation between atomic charges or spin populations and experimental isomer shifts, atomic charges did not correlate with δ^{exp} values. However, spin population values showed the negative correlation with δ^{exp} of Eu system and the positive correlation with δ^{exp} of Np system corresponding to the reversal of $(\Delta R / R)$ sign between ^{151}Eu and ^{237}Np nuclei. Since spin population originated from α-spinor in almost the number of f electrons, the variation of spin population can be regarded as the contribution of f-electrons to the electronic interaction between metal and donor atoms. These results indicated that the valence electrons contributed to Mössbauer isomer shifts, which was consistent with the calculation result that the contribution of valence electrons to ρ_0 correlated with experimental δ for ^{57}Fe benchmark study.[7] Similar results were obtained for Löwdin's population analysis (Table S4) and natural population analysis (Table S5) calculated by program *NBO 6.0*[54], implying that spin population analysis was suitable for the estimation of the bonding interaction between metal atom and ligands in Ln/An complexes.

4. Conclusions

We first performed the benchmark investigation of ^{151}Eu and ^{237}Np Mössbauer isomer shifts by means of all-electron relativistic ZORA-DFT calculation for the sake of understanding quantitatively the bonding properties of f-element compounds. Applying the all-electron relativistic DFT to ten Eu and ten Np benchmark complexes, we obtained the plausible geometries to the reported X-ray structures by the geometry optimization at ZORA-BP86 / SARC level. Benchmark

studies between the calculated electron density at nucleus position and the experimental Mössbauer isomer shifts revealed the extremely high performance of B2PLYP method, while that BP86 and B3LYP tended to overestimate the covalent interaction between metal and ligands. These results suggested that B2PLYP functional was one of the candidate to illustrate quantitatively the electron correlation in both lanthanide and actinide complexes corresponding to the covalent interaction between metal and ligands. We also showed that the Mulliken's spin population was the suitable parameter as the simple indicator to estimate the degree of the bonding interaction for f-element compounds. It is expected that the present work shines the brilliant light to f-element chemistry.

Supplementary Information

Cartesian coordinates of all calculated geometries, calculated ρ_0 values of various functionals for smaller Eu and Np benchmark set and numerical data for Mulliken's and Löwdin's population analyses.

Bibliographic references and notes

1 N. Kaltsoyannis, *Chem. Soc. Rev.*, 2003, **32**, 9.

2 G. Schreckenbach, and G. A. Shamov, *Acc. Chem. Res.*, 2010, **43**, 19.

3 C. Platas-Iglesias, A. Roca-Sabio, M. Regueiro-Figueroa, D. Esteban-Gomez, A. de Blas, and T. Rodriquez-Blas, *Curr. Inorg.Chem.*, 2011, **1**, 91.

4 G. Depaoli, U. Russo, G. Valle, F. Grandjean, A. F. Williams, and G. J. Long, *J. Am. Chem. Soc.*, 1994, **116**, 5999.

5 D. G. Karraker, J. A. Stone, *Inorg. Chem.*, 1979, **18**, 2205.

6 P. Gütlich, E. Bill, A. X. Trautwein, in *Mössbauer Spectroscopy and Transition Metal Chemistry*, ed. P. Gütlich, E. Bill, A. X. Trautwein, Springer, Berlin, Heidelberg, 2011, ch. 4, pp. 79-80.

7 Y. Zhang, J. Mao, E. Oldfield, *J. Am. Chem. Soc.*, 2002, **124**, 7829.

8 F. Neese, *Inorg. Chim. Acta*, 2002, **337**, 181.

9 Y. Zhang, E. Oldfield, *J. Phys. Chem. A*, 2003, **107**, 4147.

10 S. Sinnecker, L. D. Slep, E. Bill, F. Neese, *Inorg. Chem.*, 2005, **44**, 2245.

11 M. Römelt, S. Ye, F. Neese, *Inorg. Chem.*, 2009, **48**, 784.

12 Y. Ling, Y. Zhang, *J. Am. Chem. Soc.*, 2009, **131**, 6386.

13 A. D. Bochevarov, R. A. Friesner, S. J. Lippard, *J. Chem. Theory Comput.*, 2010, **6**, 3735.

14 G. M. Sandala, K. H. Hopmann, A. Ghosh, L. Noodleman, *J. Chem. Theory Comput.*, 2011, **7**, 3232.

15 M. Papai, G. Vankó, *J. Chem. Theory Comput.*, 2013, **9**, 5004.

16 M. Firatov, *J. Chem. Phys.*, 2007, **127**, 084101.

17 R. Kuian, M. Firatov, *J. Chem. Theory Comput.*, 2008, **4**, 278.

18 M. Filatov, *Coord. Chem. Rev.*, 2009, **253**, 594.

19 R. Kurian, M. Filatov, *Phys. Chem. Chem. Phys.*, 2010, **12**, 2758.
20 M. Filatov, W. Zou, D. Cremer, *J. Chem. Theory Comput.*, 2012, **8**, 875.
21 M. J. Tassel, N. Kaltsoyannis, *Dalton Trans.*, 2010, **39**, 6719.
22 A. Zaiter, B. Amine, Y. Bouzidi, L. Belkhiri, A. Boucekkine, M. Ephritikhine, *Inorg. Chem.*, 2014, **53**, 4687.
23 F. Neese, ORCA, version 3.0.0, Max Planck Institute for Chemical Energy Conversion, Ruhr, Germany, 2013.
24 C. van Wüllen, *J. Chem. Phys.*, 1998, **109**, 392.
25 D. A. Pantazis, F. Neese, *J. Chem. Theory Comput.*, 2009, **5**, 2229.
26 D. A. Pantazis, F. Neese, *J. Chem. Theory Comput.*, 2011, **7**, 277.
27 D. A. Pantazis, X. Chen, C. R. Landis, and F. Neese, *J. Chem. Theory Comput.*, 2008, **4**, 908.
28 D. A. Pantazis, F. Neese, *WIREs Comput. Mol. Sci.*, 2014, **4**, 363.
29 R. S. Mulliken, *J. Chem. Phys.*, 1955, **23**, 1833.
30 K. Momma, F. Izumi, *J. Appl. Crystallogr.*, 2008, **41**, 653.
31 A. F. Williams, F. Grandjean, G. J. Long, T. A. Ulibarri, W. J. Evans, *Inorg. Chem.*, 1989, **28**, 4584.
32 M. Katada, T. Ishiyama, S. Kawata, S. Kitagawa, *Conference Proceedings Vol. 50 "ICAME-95"*, ed. I. Ortalli, Sif, Bologna, 1996, p. 111.
33 K. Burger, Z. Nemes-Vetéssy, A. Vértes, E. Kuzmann, M. Suba, J. T. Kiss, H. Ebel, M. Ebel, *Struct. Chem.*, 1990, **1**, 251.
34 T. D. Tilley, R. A. Andersen, B. Spencer, A. Zalkin, D. H. Templeton, *Inorg. Chem.*, 1980, 19, 2999.
35 W. J. Evans, L. A. Hughes, T. P. Hanusa, *Organometallics*, 1986, 5, 1285.
36 S. Wang, Y. Yu, Z. Ye, C. Qian, X. Huang, *J. Organomet. Chem.*, 1994, 464, 55.
37 G. Depaoli, U. Russo, G. Valle, F. Grandjean, A. F. Williams, G. J. Long, *J. Am. Chem. Soc.*, 1994, 116, 5999.
38 J. Wang, M. Takahashi, T. Kitazawa, M. Takeda, *J. Rare Earths*, 2007, 25, 647.
39 A. L. Il'inskii, L. A. Aslanov, V. I. Ivanov, A. D. Khalilov, O. M. Petrukhin, *Russ. J. Struct. Chem.*, 1969, 10, 285.
40 Y. Zheng, L. Zhou, J. Lin, S. Zhang, *Z. Anorg. Allg. Chem.*, 2001, 627, 1643.
41 J. Lhoste, N. Henry, T. Loiseau, F. Abraham, *Polyhedron*, 2011, 30, 1289.
42 J. F. Bower, S. A. Cotton, J. Fawcett, R. S. Hughes, D. R. Russell, *Polyhedron*, 2003, 22, 347.
43 D. G. Karraker, J. A. Stone, *J. Am. Chem. Soc.*, 1976, **96**, 6885.
44 D. G. Karraker, J. A. Stone, *Inorg. Chem.*, 1972, **11**, 1742.
45 K. O. Hodgson, K. N. Raymond, *Inorg. Chem.*, 1972, 11, 3030.
46 D. J. De Ridder, J. Rebizant, C. Apostolidis, B. Kanellakopulos, E. Dornberger, *Acta Crystallogr.*,

Sect. C, 1996, 52, 597.

47 C. Wong, T. Yen, T. Lee, *Acta Crystallogr.*, 1965, 18, 340.

48 D. J. De Ridder, C. Apostolidis, J. Rebizant, B. Kanellakopulos, R. Maier, *Acta Crystallogr.*, *Sect. C*, 1996, 52, 1436.

49 J. H. Burns, *J. Organomet. Chem.*, 1974, 69, 225.

50 G. Perego, M. Cesari, F. Farina, G. Lugli, *Acta Crystallogr.*, *Sect. B*, 1976, 32, 3034.

51 R. D. Ernst, W. J. Kennelly, C. S. Day, V. W. Day, T. J. Marks, *J. Am. Chem. Soc.*, 1979, 101, 2656.

52 D. A. Shirley, *Rev. Mod. Phys.*, 1964, **36**, 339.

53 B. D. Dunlap, G. M. Kalvius, S. L. Ruby, M. B. Brodsky, D. Cohen, *Phys. Rev.*, 1968, **171**, 316.

54 E. D. Glendening, J. K. Badenhoop, A. E. Reead, J. E. Carpenter, J. A. Bohmann, C. M. Morales, C. R. Landis, F. Weinhold, NBO, version 6.0, Theoretical Chemistry Institute, University of Wisconsin, Madison, WI, 2013.

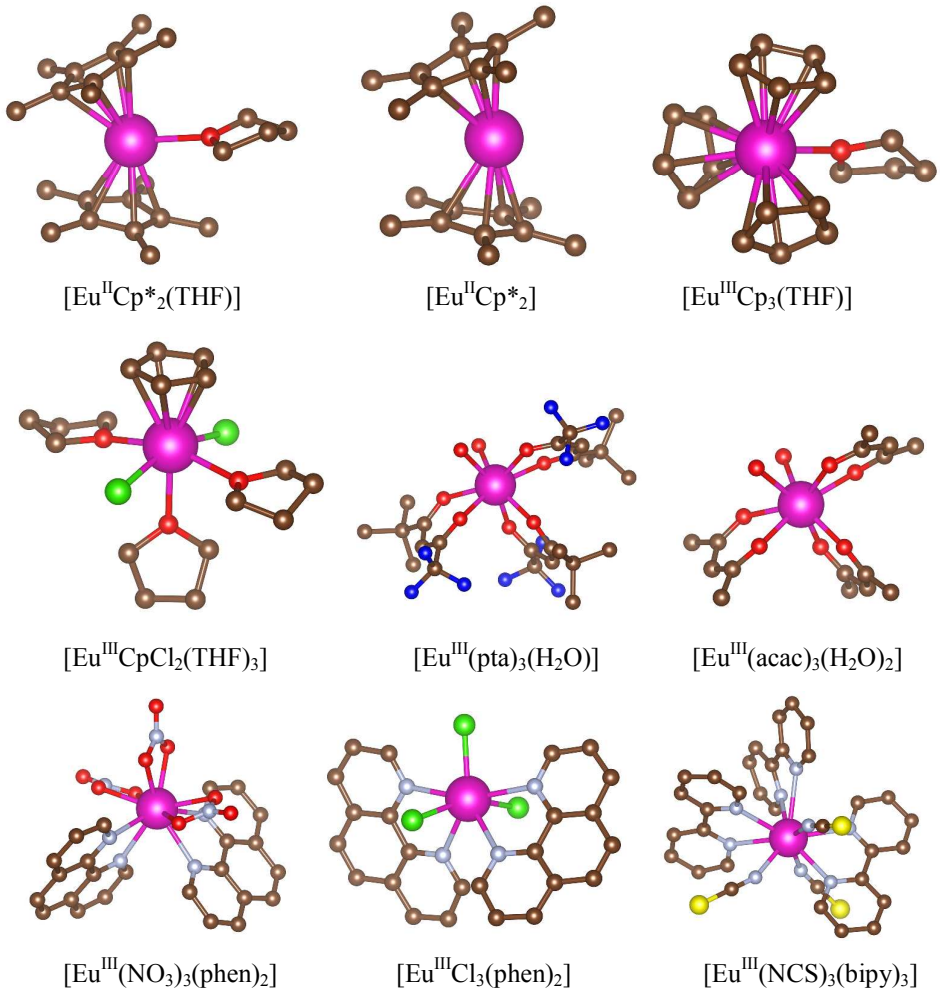

Figure 1 Equilibrium structures of Eu benchmark complexes, in which hydrogen atoms were omitted for simplicity. Purple, green, yellow, blue, red, light-blue and brown spheres represent Eu, Cl, S, F, O, N and C, respectively.

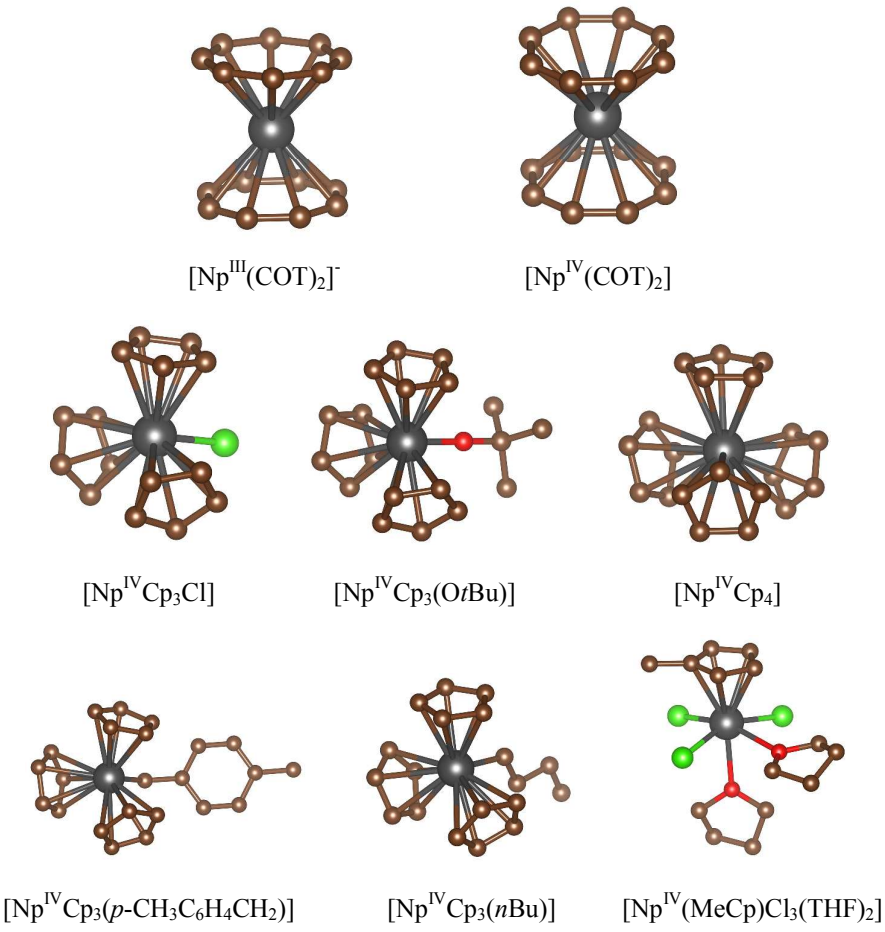

Figure 2 Equilibrium structures of Np benchmark complexes, in which hydrogen atoms were omitted for simplicity. Black, green, red and brown spheres represent Np, Cl, O and C, respectively.

(a) BP86

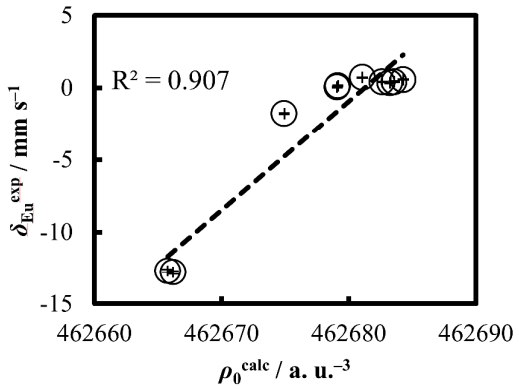

(b) B3LYP

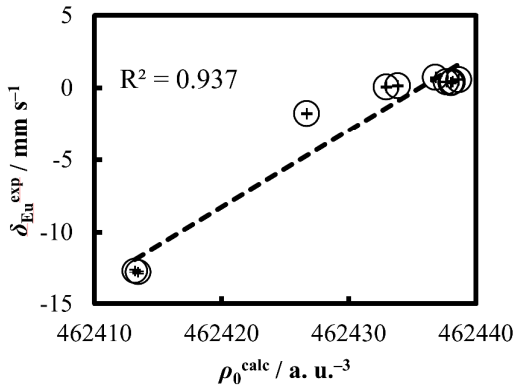

(c) B2PLYP

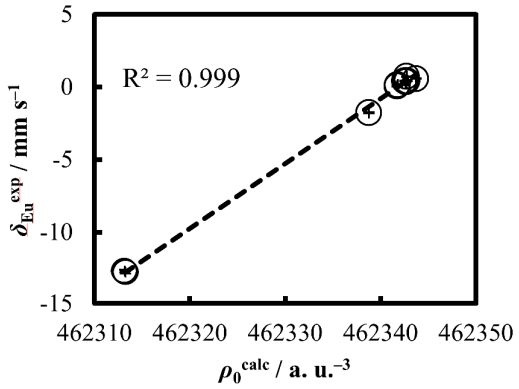

Figure 3 ^{151}Eu Mössbauer benchmark results between δ_{Eu}^{exp} and ρ_0^{calc} by each method.

(a) BP86

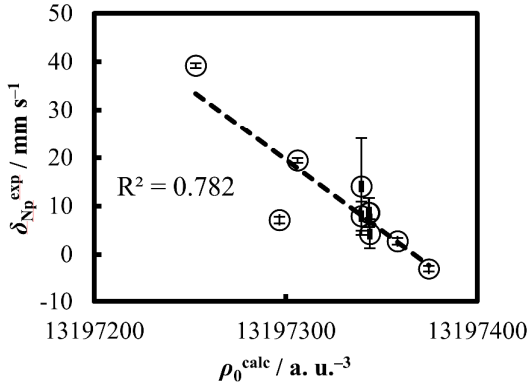

(b) B3LYP

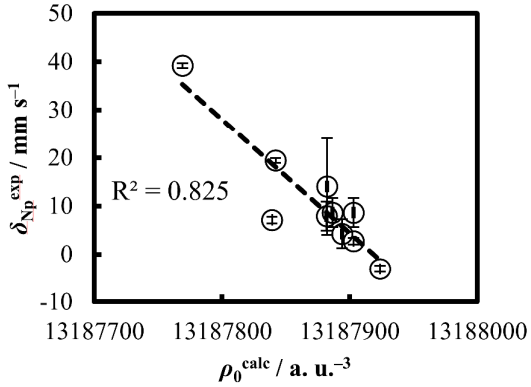

(c) B2PLYP

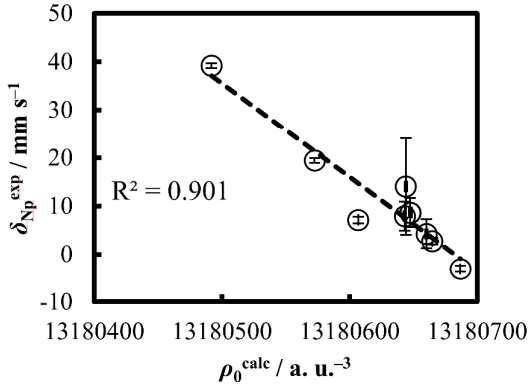

Figure 4 ^{237}Np Mössbauer benchmark results between δ_{Eu}^{exp} and ρ_0^{calc} by each method.

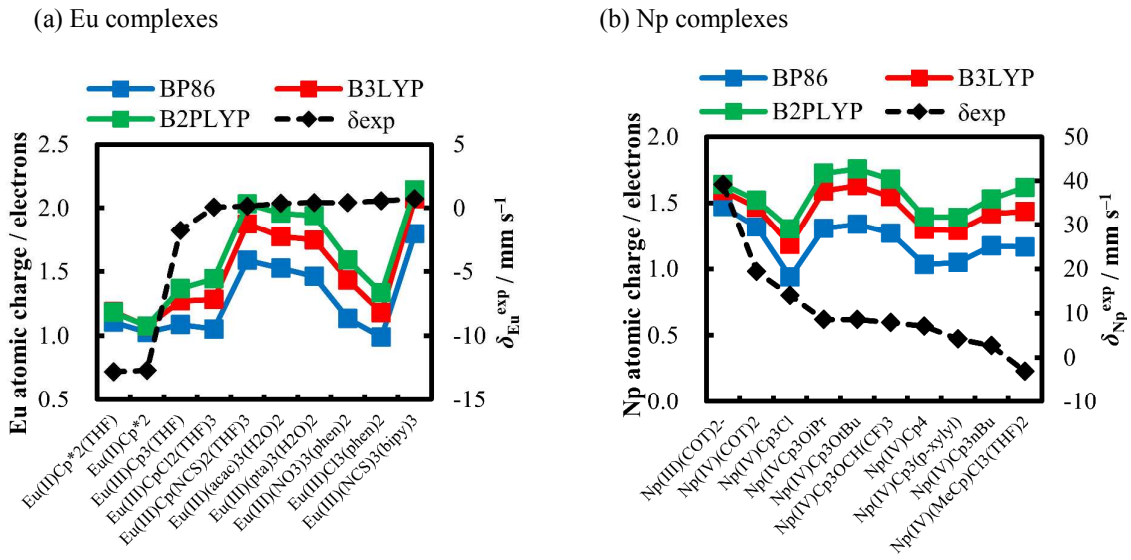

Figure 5 Comparison of Mulliken's atomic charge with δ^{exp}.

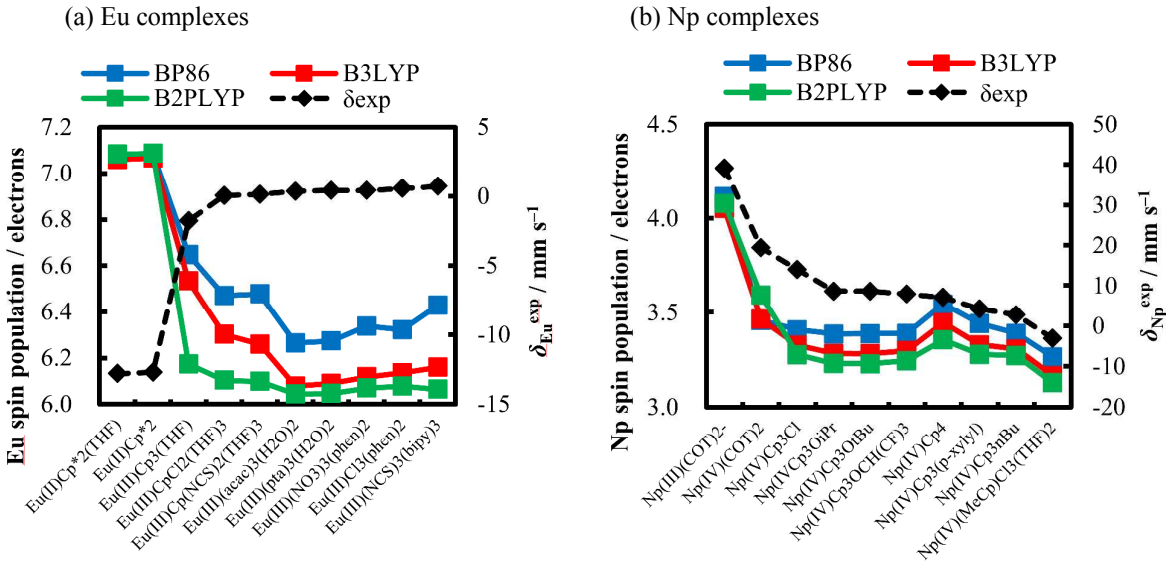

Figure 6 Comparison of Mulliken's spin population with δ^{exp}.

Table 1 Experimental isomer shifts of Eu and Np complexes employed for benchmark study

(a) Eu benchmark complexes

Eu complexes	δ_{Eu}^{exp} / mm s^{-1} [a]	Temperature / K	Ref.[b]	Ref.[c]
$[Eu^{II}Cp^*_2(THF)]$	–12.8(1)	4.2	31	34
$[Eu^{II}Cp^*_2]$	–12.7(1)	4.2	31	35
$[Eu^{III}Cp_3(THF)]$	–1.77(5)	4.2	4	36
$[Eu^{III}CpCl_2(THF)_3]$	0.06(5)	4.2	4	37
$[Eu^{III}Cp(NCS)_2(THF)_3]$	0.14(5)	4.2	4	37[d]
$[Eu^{III}(pta)_3(H_2O)_2]$	0.42(4)	4.2	32	38
$[Eu^{III}(acac)_3(H_2O)_2]$	0.36(4)	4.2	32	39
$[Eu^{III}(NO_3)_3(phen)_2]$	0.41(2)	77	33	40
$[Eu^{III}Cl_3(phen)_2]$	0.57(2)	77	33	41
$[Eu^{III}(NCS)_3(bipy)_3]$	0.72(2)	77	33	42

(b) Np benchmark complexes

Np complexes	δ_{Np}^{exp} / mm s^{-1} [e]	Temperature / K	Ref.[b]	Ref.[c]
$[Np^{III}(COT)_2]^-$	39.2(5)	4.2	43	45
$[Np^{IV}(COT)_2]$	19.4(5)	4.2	43	46
$[Np^{IV}Cp_3Cl]$	14(10)	4.2	44	47
$[Np^{IV}Cp_3\{OCH(CH_3)_2\}]$	8.6(20)	4.2	5	48[f]
$[Np^{IV}Cp_3\{OC(CH_3)_3\}]$	8.6(30)	4.2	5	48[f]
$[Np^{IV}Cp_3\{OCH(CF_3)_2\}]$	7.9(20)	4.2	5	48[f]
$[Np^{IV}Cp_4]$	7.2(2)	4.2	44	49
$[Np^{IV}Cp_3(p\text{-}CH_3C_6H_4CH_2)]$	4.2(28)	4.2	5	50
$[Np^{IV}Cp_3(n\text{-}C_4H_9)]$	2.7(7)	4.2	5	50
$[Np^{IV}(MeCp)Cl_3(THF)_2]$	–3.1(7)	4.2	5	51

Parentheses values show the experimental errors.

[a] Relative values to EuF_3

[b] Refs. for isomer shifts

[c] Refs. for X-ray structures

[d] Substituted Cl of $[Eu^{III}CpCl_2(THF)_3]$ with NCS

[e] Relative values to $NpAl_2$

[f] Substituted OPh of $[Np^{IV}Cp_3(OPh)]$ with OR (R = $CH(CH_3)_2$, $C(CH_3)_3$ and $CH(CF_3)_2$)

Table 2 Comparison of bond lengths between calculated and experimental structures for Eu benchmark complexes

Complexes	M-L	r^{calc} / Å		r^{exp} / Å	
$[M^{II}Cp^*_2]$	M-C_{ave}(Cp*)	M = Eu	2.74(1)	M = Eu	2.79[a]
$[M^{III}Cp_3(THF)]$	M-C_{ave}(Cp)	M = Eu	2.81(2)	M = Sm	2.73[b]
	M-O(THF)		2.63		2.52[b]
$[M^{III}CpCl_2(THF)_3]$	M-C_{ave}(Cp)	M = Eu	2.80(0.8)	M = Eu	2.71[c]
	M-Cl_{ave}		2.68(0.5)		2.67[c]
	M-O_{ave}(THF)		2.55(2)		2.45[c]
$[M^{III}(pta)_3(H_2O)_2]$	M-O_{ave}(pta)	M = Eu	2.39(5)	M = Gd	2.39[d]
	M-O_{ave}(H_2O)		2.54(2)		2.45[d]
$[M^{III}(acac)_3(H_2O)_2]$	M-O_{ave}(acac)	M = Eu	2.40(4)	M = Eu	2.43[e]
	M-O_{ave}(H_2O)		2.57(2)		2.56[e]
$[M^{III}Cl_3(phen)_2]$	M-Cl_{ave}	M = Eu	2.65(0.4)	M = Eu	2.63[f]
	M-N_{ave}(phen)		2.67(0.6)		2.61[f]

Parentheses values show the standard errors to average lengths.

[a] Ref. 35

[b] Ref. 36

[c] Ref. 40

[d] Ref. 38

[e] Ref. 39

[f] Ref. 41

Table 3 Comparison of bond lengths between calculated and experimental structures for Np benchmark complexes

Complexes	M-L	r(M-L)^{calc} / Å		r(M-L)^{exp} / Å	
$[M^{III}(COT)_2]^-$	M-C_{ave}(COT)	M = Np	2.72(0.2)	M = Ce	2.71[a]
$[M^{IV}(COT)_2]$	M-C_{ave}(COT)	M = Np	2.68(0.7)	M = Np	2.63[b]
$[M^{IV}Cp_3Cl]$	M-C_{ave}(Cp)	M = Np	2.76(1)	M = U	2.74[c]
	M-Cl		2.60		2.56[c]
$[M^{IV}Cp_4]$	M-C_{ave}(Cp)	M = Np	2.85(2)	M = U	2.81[d]
$[M^{IV}Cp_3(p\text{-}CH_3C_6H_4CH_2)]$	M-C_{ave}(Cp)	M = Np	2.76(2)	M = U	2.71[e]
	M-C(*p*-xylyl)		2.48		2.54[e]
$[M^{IV}Cp_3(n\text{-}C_4H_9)]$	M-C_{ave}(Cp)	M = Np	2.77(1)	M = U	2.73[e]
	M-C(*n*Bu)		2.44		2.43[e]
$[M^{IV}(MeCp)Cl_3(THF)_2]$	M-C_{ave}(Cp)	M = Np	2.73(1)	M = U	2.72[f]
	M-Cl_{ave}		2.61(2)		2.62[f]
	M-O_{ave}(THF)		2.56(2)		2.45[f]

Parentheses values show the standard errors to average lengths.

[a] Ref. 45

[b] Ref. 46

[c] Ref. 47

[d] Ref. 49

[e] Ref. 50

[f] Ref. 51

Table 4 Calculated electron densities at nucleus and isomer shifts and fit parameters (a, b) according to Eq. 2 for the Eu benchmark set

Eu complexes	δ^{exp} / mm s^{-1}	BP86		B3LYP		B2PLYP	
		ρ_0^{calc} / a.u.$^{-3}$	δ^{calc} / mm s^{-1}	ρ_0^{calc} / a.u.$^{-3}$	δ^{calc} / mm s^{-1}	ρ_0^{calc} / a.u.$^{-3}$	δ^{calc} / mm s^{-1}
[Eu^{II}Cp*$_2$(THF)]	–12.8(1)	462666.187	–11.35	462413.440	–11.76	462313.262	–12.74
[Eu^{II}Cp*$_2$]	–12.7(1)	462665.761	–11.67	462413.186	–11.89	462313.149	–12.79
[Eu^{III}Cp$_3$(THF)]	–1.77(5)	462674.919	–4.77	462426.701	–4.71	462338.763	–1.36
[Eu^{III}CpCl$_2$(THF)$_3$]	0.06(5)	462679.088	–1.63	462432.949	–1.40	462341.734	–0.04
[Eu^{III}Cp(NCS)$_2$(THF)$_3$]	0.14(5)	462679.142	–1.59	462433.858	–0.91	462341.774	–0.02
[Eu^{III}(pta)$_3$(H$_2$O)$_2$]	0.42(4)	462683.579	1.76	462438.165	1.37	462342.784	0.43
[Eu^{III}(acac)$_3$(H$_2$O)$_2$]	0.36(4)	462683.225	1.49	462438.041	1.31	462342.645	0.37
[Eu^{III}(NO$_3$)$_3$(phen)$_2$]	0.41(2)	462682.619	1.03	462437.676	1.11	462342.545	0.32
[Eu^{III}Cl$_3$(phen)$_2$]	0.57(2)	462684.269	2.28	462438.652	1.63	462343.695	0.84
[Eu^{III}(NCS)$_3$(bipy)$_3$]	0.72(2)	462681.071	–0.13	462436.826	0.66	462342.724	0.40
a / mm s^{-1} a.u.^{3}		0.754		0.531		0.446	
b / a.u.$^{-3}$		462681.249		462435.581		462341.818	
RMSD / mm s^{-1}		1.584		1.307		0.198	
Correlation coefficient (r)		0.952		0.968		0.999	

Table 5 Calculated electron densities at nucleus and isomer shifts and fit parameters (a, b) according to Eq. 2 for the Np benchmark set

Np complexes	δ_{Np}^{exp} / mm s^{-1}	BP86		B3LYP		B2PLYP	
		ρ_0^{calc} / a.u.$^{-3}$	δ_{Np}^{calc} / mm s^{-1}	ρ_0^{calc} / a.u.$^{-3}$	δ_{Np}^{calc} / mm s^{-1}	ρ_0^{calc} / a.u.$^{-3}$	δ_{Np}^{calc} / mm s^{-1}
$[Np^{III}(COT)_2]^-$	39.2(5)	13197253.055	33.40	13187769.138	35.30	13180491.943	37.07
$[Np^{IV}(COT)_2]$	19.4(5)	13197306.306	17.79	13187842.138	18.07	13180572.760	21.35
$[Np^{IV}Cp_3Cl]$	14(10)	13197339.616	8.03	13187882.414	8.56	13180644.139	7.46
$[Np^{IV}Cp_3\{OCH(CH_3)_2\}]$	8.6(20)	13197343.619	6.85	13187886.648	7.56	13180647.797	6.75
$[Np^{IV}Cp_3\{OC(CH_3)_3\}]$	8.6(30)	13197343.288	6.95	13187903.265	3.64	13180647.573	6.79
$[Np^{IV}Cp_3\{OCH(CF_3)_2\}]$	7.9(20)	13197339.563	8.04	13187882.140	8.62	13180643.344	7.61
$[Np^{IV}Cp_4]$	7.2(2)	13197296.747	20.59	13187839.345	18.73	13180606.834	14.72
$[Np^{IV}Cp_3(p\text{-}CH_3C_6H_4CH_2)]$	4.2(28)	13197344.031	6.73	13187894.290	5.76	13180660.313	4.31
$[Np^{IV}Cp_3(n\text{-}C_4H_9)]$	2.7(7)	13197358.411	2.52	13187903.265	3.64	13180664.857	3.43
$[Np^{IV}(MeCp)Cl_3(THF)_2]$	–3.1(7)	13197374.832	–2.30	13187924.087	–1.28	13180686.967	–0.88
a / mm s^{-1} a.u.^{3}		–0.293		–0.236		–0.195	
b / a.u.$^{-3}$		13197366.992		13187918.672		13180682.464	
Root mean square error / mm s^{-1}		5.166		4.633		3.484	
Correlation coefficient (r)		–0.884		–0.908		–0.949	

Benchmark study of Mössbauer isomer shifts of Eu and Np complexes by relativistic DFT calculation for the understanding of bonding nature of f-block compounds

Masashi Kaneko,[a] Sunao Miyashita,[a] and Satoru Nakashima*[b]

Ten Eu and ten Np benchmark complexes were calculated by relativistic all-electron DFT including scalar-relativistic ZORA Hamiltonian and spin-orbit coupling. B2PLYP functional gave a good correlation with Mössbauer experiment for both Eu and Np systems.

Graphical Abstract